IPPI

Polyolefins Journal, Vol. 4, No. 1 (2017)
DOI: 10.22063/poj.2016.1371

REVIEW PAPER

Electrical and electromagnetic properties of isolated carbon nanotubes and carbon nanotube-based composites

Alireza Nikfarjam[1*], Roham Rafiee[2], Mostafa Taheri[2]

[1]Department of MEMS&NEMS, Faculty of New Sciences and Technologies, University of Tehran, P.O.BOX:14395-1561, Tehran, Iran
[2]Composites Research Laboratory, Faculty of New Sciences and Technologies, University of Tehran, Tehran 1439955941 Iran

Received: 15 March 2016, Accepted: 21 July 2016

ABSTRACT

Isolated carbon nanotubes (CNTs), CNT films and CNT-polymer nanocomposites are a new generation of materials with outstanding mechanical, thermal, electrical and electromagnetic properties. The main objective of this article is to provide a comprehensive review on the investigations performed in the field of characterizing electrical and electromagnetic properties of isolated CNTs and CNT-reinforced polymers either theoretically or experimentally. The results reported in literature are reviewed and evaluated based on employed and/or developed methods by focusing on the electrical conductivity, permittivity and permeability properties. Available analytical and numerical simulations for predicting electrical properties of CNT-based composites are also reviewed. Besides, equivalent circuit modeling of nanocomposites containing CNTs is presented. The influence of effective parameters on overall electrical and electromagnetic characteristics of CNT-reinforced polymers is discussed based on published data. Therefore, highlighting the recent trends and challenges engaged in new investigations, those aspects which are required to be more deeply explored are introduced. **Polyolefins J (2017) 4: 43-68**

Keywords: Carbon nanotubes; nanocomposite; electrical properties; permittivity; permeability.

CONTENT

* Corresponding Author - E-mail: a.nikfarjam@ut.ac.ir

INTRODUCTION

Carbon nanotubes (CNTs) as a new generation of materials have unique mechanical, thermal, electricaland electromagnetic properties [1-6]. Carbon nanotubes in semiconducting (zigzag) and metallic (armchair) types are considered as promising reinforcements for improving the properties of polymers. By incorporating CNTs into polymers, new category of nanocomposites with improved properties can be achieved not only from mechanical point of view but also from electrical and electromagnetic aspects.

The main objective of this article is to review the researches that conducted on the field of electrical and/or electromagnetic properties of CNT-reinforced polymers through analyzing electrical conductivity, permittivity and permeability of CNT-based films and composites.These parameters have a direct influence on determining the key parameters such as reflection and transmission coefficients of microwave [7], loss tangent [8] and skin depth [9].They are important especially in high-frequency applications. Since simulation techniques including molecular dynamic (MD), Brownian dynamics (BD) and electrical circuit modeling approach are a challenging task to characterize the electrical behavior of CNT-based composites, experimental methods have been widely used by researchers [10-14].

Electrical properties of carbon nanotube can be exploited in various applications like display devices [15], batteries [16], fuel cells [17], super capacitors [18], solar cells [19] and transistors [20]. Due to their outstanding electromagnetic properties, they are also employed for constructing microwave lenses, waveguide and antennas [21], electromagnetic shielding [4-6, 22-27] and microwave absorption films [28,29,26]. Consequently, correct understanding of their functionality in electric and electromagnetic fields plays an important role in their development steps for their future potential applications.

In this article, first of all, the morphology and nanostructure of CNTs are explained and then the basic framework of electromagnetic properties is outlined. Different theoretical modeling and simulation methods for extracting electrical properties of individual CNTs and CNT-reinforced polymers are introduced afterward. Experimental measurements reported in the literature are reviewed and the trend of results is discussed by focusing on the electrical conductivity, permittivity and permeability properties.

CNT AND CNT-BASED COMPOSITES

A carbon nanotube (CNT) can be schematically considered as a rolled graphene sheet with a hexagonal lattice structure consisting of carbon atoms. In carbon nanotubes, each carbon atom is connected by covalent bonds to three other adjacent carbon atoms. Some researchers reported that the outermost wall of a MWCNT is responsible for its electrical conductivity. But recently it is reported that all walls contribute to the electrical properties of MWCNT [30,31]. MWCNTs always show metallic behavior and have diameters between several nanometers to tens of nanometers and their lengths are larger than 100 nm [32], but SWCNTs can show either metallic (Figure 1, B (right)) or semiconducting (Figure 1, B (left)) behavior according to their chirality (Figure 1, A) [33].

New generation of nanocomposites is created by incorporation of CNTs into polymeric matrices. Both thermosetting and thermoplastic resins are used for this purpose. Thermoplastic polymers include polypropylene, polystyrene, polyethylene, poly (methyl methacrylate), polycarbonate and nylon. Thermosetting polymers include polyester, vinyl ester, epoxy, phenolic, polyimide, polyurethane and silicone. Also polymers in terms of electrical properties are divided into two kinds of conductive and insulator polymers. Carbon nanotubes are employed to improve the electrical properties of insulating polymers such as PU, PEMA, PMMA, PC, epoxy, vinyl ester, PS, PVA,

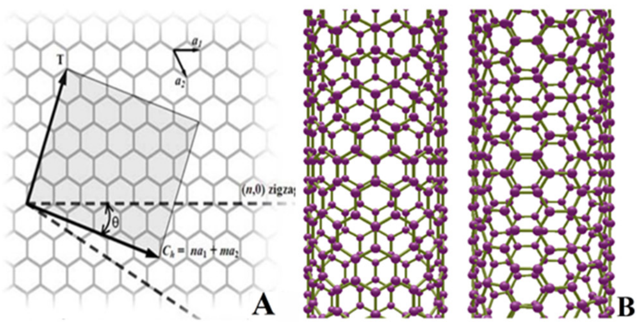

Figure 1. (A) Chirality vector of carbon nanotubes, (B) Armchair structure (6, 6) and Zigzag (12, 0) respectively, from right to left [33].

PCL, PI or even conductive polymers such as PANI, PPY, PEDOT-PSS.

ELECTROMAGNETIC AND ELECTRICAL PARAMETERS

Those characteristic parameters defining electrical and electromagnetic properties of a material are briefly explain in this section.

Electrical conductivity

Electrical conductivity is a parameter showing ability of passing the electrical current through the material. Electrical conductivity is formed in two forms, direct current (without frequency-dependent sources) and alternating current (dependent to frequency). Microwave electrical conductivity is calculated using the permittivity according to equation 1:

$$\sigma_{mw}=2\pi f\varepsilon_o\varepsilon'' \qquad (1)$$

where σ_{mw} is the electric conductivity (S/m), f is the frequency (Hz), ε_o is the vacuum permittivity (ε_o = 8.854 × 10^{-12} F/m) and ε″ is the imaginary permittivity. Microwave electrical conductivity (σ_{mw}) which is sum of the direct current (DC) and alternating current (AC) is expressed by equation 2:

$$\sigma_{mw}=\sigma_{ac}+\sigma_{dc} \qquad (2)$$

By using dielectric relaxation spectroscopy (DRS) technique the response of the system is taken through placing the samples between two capacitor plates and the applying alternating voltage [34]. By measuring complex impedance Z* = Z' –iZ" , complex permittivity can be obtained according to equation 3 [35]:

$$\varepsilon^*(\omega)=\frac{1}{i\omega Z^*(\omega)C_o} \qquad (3)$$

Where ($\omega=2\pi f$) is the angular frequency and C_o is the equivalent capacitance of the free space[14].

With increasing CNT content in a polymer matrix, a sharp rise in conductivity of nanocomposite is observed at a specific CNT content. This is known as percolation, implying on formation of a 3Delectrically conducting network within the polymer matrix. The percolation threshold can be calculated by plotting the electrical conductivity versus the volume fraction of CNTs and fitting with a power law function [36,10,11],$\sigma = \sigma_o(\upsilon - \upsilon_o)^\beta$, where σ is the electrical conductivity of the composite, σo is the specific conductivity, υ is the volume fraction of CNTs, υ_0 is the volume fraction at the percolation threshold and β is a parameter related to the system dimensionality.

Although the lowest percolation thresholds in the CNT-based composites have been almost obtained by using the solution method [23], the percolation threshold achieved by in-situ polymerization method is about 0.0025 [11].

Permittivity

Complex permittivity (ε) is defined as the product of the relative permittivity multiplied by the vacuum permittivity constant (ε_o= 8.85×10^{-12} F/m). In equation 4, ε, D and E are the electric permittivity, electric flux density (q/m^2) and electric field intensity (v/m), respectively.

$$D = \varepsilon E \qquad (4)$$

Complex relative permittivity (ε_r) consists of two real and imaginary parts. The real part (ε') is known as dielectric constant or charge storage and the imaginary part (ε") is known as dielectric losses or loss factor (ε_r = ε' - jε"). The imaginary part indicates the ability of material in absorption of radio frequency waves. So, high value of this parameter (loss factor), indicates materials with high absorption properties.

Permittivity at the megahertz-range frequency has high values [7] and at the gigahertz-range frequency is greatly reduced [8]. In general, permittivity always decreases by increasing the frequency. This performance occurs at high CNT volume fractions. It was shown that the real and imaginary parts of the electrical conductivity affect this parameter. Finally, for nanocomposites with higher electrical properties, the lower permittivity, especially in its imaginary part is required.

Permeability

The complex permeability (μ), as shown in equation 5, is expressed as the product of the relative permeability (μ_r) multiplied by the vacuum permeability

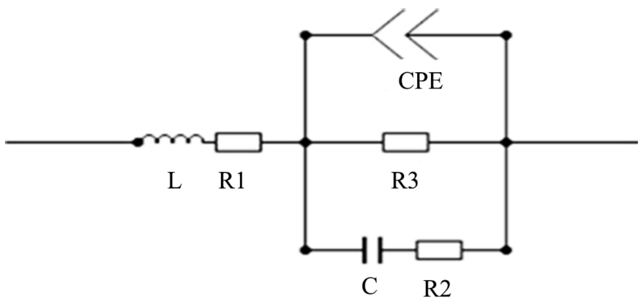

Figure 2. The equivalent circuit model of the t-MWCNT/EP and m-MWCNT/EP composites [54].

(μ_0=4π×10^{-7}H/m). Complex relative permeability (μ_r) consists of two real and imaginary parts. The real part (μ') is known as magnetic storage and the imaginary part (μ'') is known as magnetic loss (μ_r = μ' - jμ'').

$$B = \mu H \tag{5}$$

where, B is the magnetic flux density (Tesla) and H is the electric field intensity (A/m).

For enhancing microwave absorption, the initial permeability (μ_i) of the absorbing material should address the highest possible value. For example, the μ_i of ferromagnetic materials could be expressed as $\mu_i = \frac{M_S^2}{akH_C MS + b\lambda\xi}$,where a and b are constants obtained by the material compositions, λ is the magnetostriction constant, ξ is the elastic strain characteristic of the crystal, and k is a proportionality coefficient. As it can be seen, the permeability can be enhanced either by improving M_s or by decreasing H_c. This is favorable for enhancing the microwave absorption capability of the material [37].

Loss tangent

Loss tangent, known as dielectric loss or tan δ, is described by equation 6; this parameter represents the ability of converting the stored energy in the material to heat energy. High loss factor (ε″) and high loss tangent (tan δ) show high ability of the materials in absorbing the radio waves [38].

$$\tan\delta = \frac{\varepsilon''}{\varepsilon'} = \sigma\varepsilon_0\varepsilon_r \tag{6}$$

Materials with tan(δ)>>1 are known as good conductors, and with tan(δ)<<1 are known as poor conductors[39].

When the electromagnetic radiation encounters with a conductor/insulator composite surface, the electric field produces two different electric currents (conduction current and displacement current) in the material. These currents increase the loss factor (imaginary part of the permittivity). In general, absorbing the electromagnetic radiations and converting these waves into heat, depends on the complex relative permittivity and loss tangent [40]. The loss tangent or dielectric loss factor increases in CNT-based composites by increasing the diameter and volume fraction of CNT.

Skin depth

The skin depth is a distance evaluating ability of theelectromagnetic field to propagate within a material [41]. From theoretical point of view, a good conductor has zero skin depth. While for aluminum, this distance is placed between 0.748 to 0.611 μ_m for the Ku frequency band (12 to 18 GHz) at μ_r=1 and resistivity of 2.65×10^{-8} (Ωm). Skin depth is calculated using below equation:

$$\delta = \sqrt{\frac{2}{\omega.\mu.\sigma}} = \sqrt{\frac{2}{\pi.f.\mu}} \tag{7}$$

where ρ is the resistivity of the conductor in Ω.m, f is the frequency in Hz and μ is the absolute magnetic permeability of the conductor.

THEORETICAL METHODS OF OBTAINING ELECTRICAL PROPERTIES OF ISOLATED CNTs AND NANOCOMPOSITES CONTAINING CNTs

In a general classification, the electrical properties have been extracted by both the theoretical and experimental methods. In this section, the theoretical methods categorized under simulations and modeling techniques are introduced.

Molecular dynamics simulations (MD)

In molecular dynamics simulations (MD) and Brownian dynamics simulations (BD), the simulation of carbon-carbon bonds of one or several carbon nanotubes is explained. Although these methods are very accurate in prediction, they are suffering from complex formulations, intensive computations and considerable simulation runtimes. They are able only to compute the limited lengths of carbon nanotubes [42].

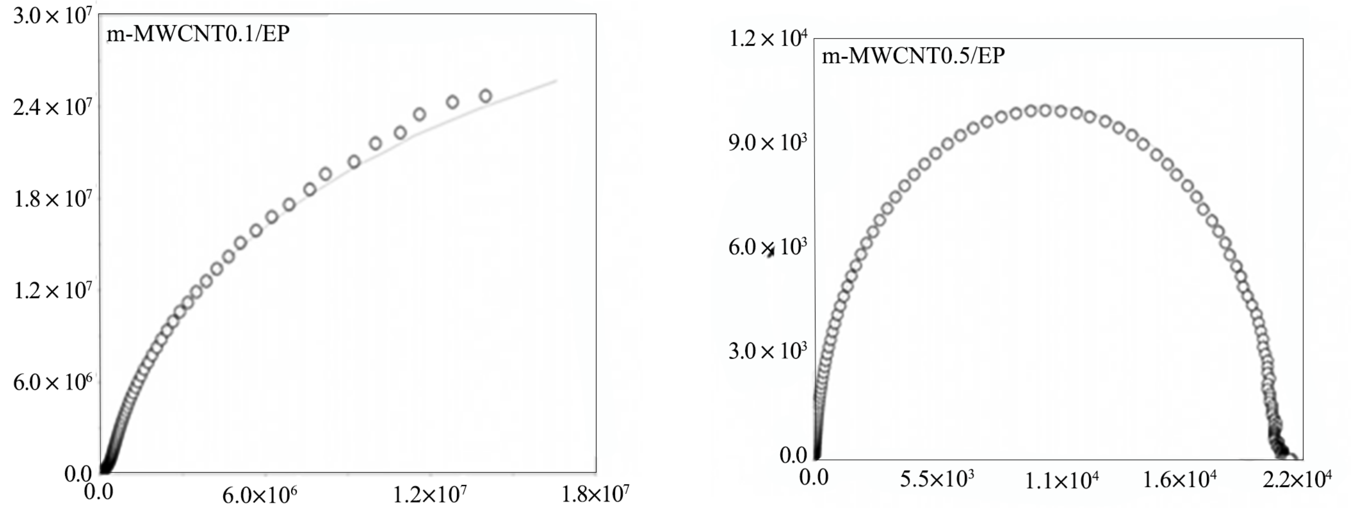

Figure 3. Impedance Nyquist plot for nanocomposites with 0.1 vol% (left) and 0.4 vol% (right) of CNT [54].

This limitation avoids to simulate the nanocomposites and ultimately their properties with broader perspectives. As it is observed in Table 4, in most of the simulation methods, the physical (mechanical) properties have been studied.

MODELING

Modeling methods are divided into three categories as: modeling of interconnections of CNTs, modeling of nanocomposites containing CNTs and probabilistic methods.

Modeling of interconnections of CNTs

In the approach of modeling of interconnections of CNTs, the models have been obtained based on existed theories for making the models. In this type of modeling, the primary data and design assumptions are extracted from MD simulation. For instance, parameters such as mean free path (MFP) (which is considered as 1.6 µm in this type of modeling) and also the van der Waals gap between shells (which is equal to 0.34 nm in modeling) are extracted from MD simulation. Although the accuracy of the modeling methods is lower than that of the MD simulation, they are not limited to small systems and through presenting some proofs and assumptions all types of single, double and multi-walled CNTs and also bundle of CNTs can be modeled.

In all contents related to polymer-based nanocomposites, the data have been collected based on the results extracted from tests on different combinations. Burke studied on the electrical properties of nanotubes at high frequency by extracting the electrical equivalent circuit of single wall carbon nanotubes [43, 44]. Within the recent decade, considering the simple structure of single wall carbon nanotubes comparing to double and multiwall ones, these types of carbon nanotubes have received more attentions. Considerable advancements in this context ultimately resulted in accessing to functional specifications of a single wall carbon nanotube and bundle of single wall carbon nanotubes [44, 45]. For instance, researches have been performed to establish equivalent circuit of a SWCNT [44, 46] and ultimately resulted in functional predictions of SWCNT connections [44]. In some papers, the dependence of nanotubes diameter for connection and Ohmic resistances of a bundle of SWCNT which are very important for implementation of nanotubes connections, have been evaluated [47]. The maximum value of conductive channel per cross-section area is required to reach the maximum conductivity in the applications of CNTs interconnections. Naeemi and Meindl [45] examined and calculated the number of conductive channels available in MWCNT by the approximate method and also presented a physical model of MWCNT.

Higher diameters of MWCNTs will be led to higher electrical performance [46, 47]. Puet al. [48] have constructed the electrical model of DWCNT interconnections. DWCNTs have a simpler structure than

MWCNTs, because the van der Waals force within the gap between two shells remains in the constant value. In DWCNTs, the diameter of internal shell is different from that of external shell; therefore their resistances will be different from each other.

The recent tests show that the resistance of a MWCNT [49] or bundle of MWCNTs [50] may be lower than that of an ideal conductor SWCNT, and also it is evident that more than one wall is effective in defining their conductivity.

Electrical conductivity of a CNT is described by equation 8:

$$G = G_0 = (2e^2/h)M \tag{8}$$

In the above equation, $G_0 = (2e^2/h) = (12.9k\Omega)^{-1}$, e is the electron charge; h is Planck's constant and M is the number of available conductive channels.

Electrical conductivity and resistance of all types of CNTs which have been obtained using theoretical modeling are tabulated in Table 1 [51-53].

Modeling of nanocomposites containing CNTs

The second category of modeling that is known as semi-empirical modeling is dealing with modeling of all types of nanocomposites containing CNTs. Electrochemical impedance spectroscopy (EIS) is an analytical method for investigating the properties of numerous complex nonlinear electrochemical processes with different conditions (such as temperature, pressure, etc.) that uses relatively simple equivalent circuits (consist of resistance, inductor and capacitor). Ultimately, upon drawing the Nyquist impedance diagram and extraction of corresponding data, the respective electrical model will be extracted.

Cheng et al. [54] presented an electrical equivalent circuit model of nanocomposites containing MWCNT and epoxy with use of semi-empirical method shown in Figure 2.

Results proved that the simulated impedance spectra of the equivalent circuit (see Figure 2) fitted the actual impedance spectra of composites (Figure 3). Then Figure 2 could be confirmed as the equivalent circuit model of the composites prepared herein. Specifically, the equivalent circuit consists of a capacitance (C), an inductance (L), a constant phase element (CPE) and three resistances (R1, R2, and R3). Because the t-MWCNT/EP and m-MWCNT/EP composites have similar microstructures, so they have similar equivalent circuit elements [54].

The corresponding parameters from the equivalent circuit model have been calculated and shown in Table 2.

The impedance Nyquist plot obtained from EIS includes a circular part and an inclined line. This type of plot (plot with one time constant) is simulated by the simple electrical circuits. In Figure 4, the impedance Nyquist plots are shown for the specimens containing 0.1 and 3 wt% of MWCNT [55].

The electrical equivalent circuit extracted from the impedance plots is depicted in Figure 5. This equivalent circuit comprises of four electrical elements including solution resistance, charge transfer resistance, double-layer capacitance and Warburg impedance.

The numerical values of electrical equivalent circuit elements presented for the investigated nanocomposites are presented in Table 3 for different wt% of CNT and in the frequency range of 101 to 108 Hz.

Modeling based on probabilistic methods

In these methods, the distortion of carbon nanotubes and their effects are studied. The distortion which is arisen from the aspect ratio of the nanotubes in the resin causes to create more connection points compared to those created in straight nanotubes. This will change the connection resistance. Lithium and Thostenson [56] presented a probabilistic model and studied the distortion of nanotubes and the effect of this parameter on the percolation threshold and electrical conductivity. They generated a network of carbon nanotubes randomly in the form of long polygons with the equal lengths in a rectangular shape with the specified length and width and considered a random direction for each situation. They also studied the impact of aspect ratio and curvature of nanotubes. Yi et al. [57] modeled the nanotubes as sinusoidal waves in their modeling.

In Table 4, samples of theoretical (simulation, modeling) and experimental methods are provided [8, 10-19, 21, 34, 41, 42, 44, 54, 56-58]. Mendes et al. [58] used Brownian dynamics simulation for separation of the conductive and semi-conductive carbon nanotubes.

Table 1. Electrical conductivity and resistance of CNTs in theoretical method.

Researcher	Material	Chirality	Aspect ratio	Diameter (nm)	Length (μm)	Resistance (kΩ)	Conductivity (s/m)	Year
Bockrath et al.[51]	Cu	-	2	14	0 to 1000	-	1227	2008
				22			1664	
				32			2070	
	SWCNT	Random (1/3 Metallic)	2	1		-	909 to 2857	
		All Metallic		1			2857 to 8333	
	MWCNT	-	2	14		-	175 to 8000	
				22			189 to 6250	
				32			227 to 5000	
Naeemi et al.[52]	Cu	-	-	14	0.1 to 1000	-	0.1×10^4	2008
				22			0.6×10^4	
				50			0.21×10^4	
				100			0.271×10^4	
	SWCNT		-	1		-	0.017×10^4 to 0.6×10^4	
							0.003×10^4 to 0.2×10^4	
				1.5				
	-----			10		-	0.006 to 0.32	
				20			0.006 to 0.6	
				50			0.006 to 1.6	
				100			0.006 to 2	
Hosseini et al.[53]	SWCNT Bundle 27 °C	Random (1/3 Metallic)	-	2.4	10 to 80 nm length of bundle	780 to 20	-	2010
				1		475 to 10		
		All Metallic		2.4		300 to 5		
				1		165 to 2.5		
	Copper Interconnect 27 °C	-	-	-	10 to 80 nm length of bundle	740 to 10	-	
	SWCNT Bundle 100 °C	Random (1/3 Metallic)	-	2.4	10 to 80 nm length of bundle	1400 to 25	-	
				1		775 to 20		
		All Metallic		2.4		470 to 10		
				1		265 to 5		
	Copper Interconnect 100 °C	-	-	-	10 to 80 nm length of bundle	760 to 20		

LITERATURE REVIEW ON EXPERIMENTAL OBSERVATIONS

Numerous researches on extracting electrical properties are devoted to the experimental methods. Experimental methods investigate parameters such as, type, geometry and structure of CNTs in isolated CNTs, and in combination of polymer and CNT. CNT volume fraction, orientation, polymer type, method of processing, disentanglement of CNT agglomerates and CNTs connection in the solution (conductive network) are also analyzed by various investigations. The electrical conductivity, permittivity, permeability, loss

Table 2. The corresponding parameters from the equivalent circuit model.

Composite	L (H)	R1 (Ω)	C (F)	R2 (Ω)	CPE (F)	n	R3 (Ω)
m-MWCNT0.5/EP	2.03×10^{-13}	5.099	5.108×10^{-12}	4436	1.955×10^{-10}	0.9204	2.407×10^{4}
t-MWCNT0.5/EP	1.378×10^{-16}	3.888	1.192×10^{-11}	2.204×10^{-12}	1.202×10^{-10}	0.9653	2.397×10^{4}

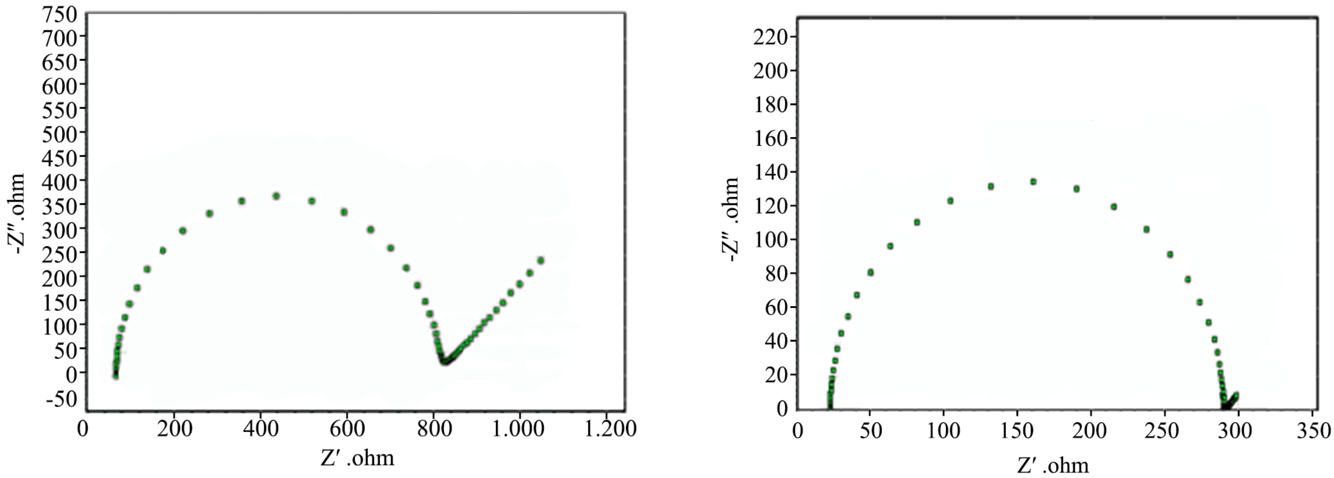

Figure 4. Impedance Nyquist plot for nanocomposites with 0.1 wt% (left) and 3 wt% (right) of CNT [55].

tangent and skin depth of CNT-reinforced polymers are investigated.

Electrical conductivity

Electrical conductivity of isolated carbon nanotubes

Among other materials, CNTs have the highest electrical conductivity [33, 59, 60]of about 109 A/cm^2 and 1010A/cm^2 at 250°C [61]. A ballistic transport phenomenon is experienced by metallic CNTs. The travelling of metal electrons is slowed down, since they are colliding with the crystal lattice and other electrons. This process is also called scattering. The average distance which can be travelled by the electron (before scattering occurs) is called the mean free path (MFP). Finally, this process will be led to Ohm's law [62]:

$$J = \sigma E \tag{9}$$

where, J is the current density, σ the electrical conductivity and E the electric field. The electrical resistance is shown by equation 10:

$$R = l\, \rho / A \tag{10}$$

where l is the length (cm), A is the cross section (cm^2) and ρ is the resistivity (Ω.cm) of the material. Finally, electrical conductivity can be obtained by reversing the resistivity, according to equation 11:

$$\rho = 1/\sigma \tag{11}$$

Reported experimental observations in literature for the electrical conductivity of isolated carbon nanotubes [63-66] and graphenes [67] are shown in Table 5. As it can be seen from Table (5), there is as light difference between electrical conductivity of steel nanoparticles [68] as a strong conductor of electrical current and carbon nanotubes [65, 66].

In Table 6 general overview of experimental observations of DC electrical conductivity of CNT-based composites are given [8-14,21,34,63,64,75-122].

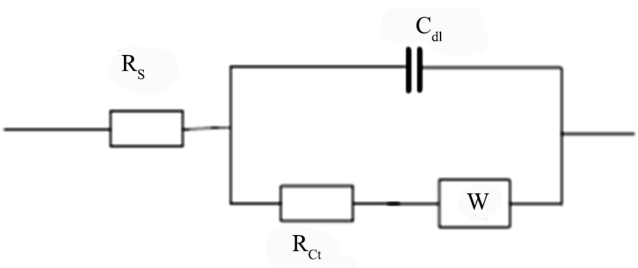

Figure 5. Electrical equivalent circuit extracted from impedance plots [55].

Table 3. Numerical values of electrical equivalent circuit elements [55].

CNTs wt%	C_{dl}	R_{ct}	R_s	Warburg coefficient
0.1	1.5×10^{-7}	742	67	5×10^{-3}
0.3	3×10^{-7}	512	48	5×10^{-2}
0.2	8×10^{-7}	438	42	1.8×10^{-2}
1	3.4×10^{-8}	345	36	3×10^{-2}
1.5	4.1×10^{-8}	327	32	5.78×10^{-2}
2	6.34×10^{-8}	290	27	7.38×10^{-2}
2.5	7.14×10^{-8}	276	25	8.09×10^{-2}
3	8.42×10^{-8}	268	22	9.12×10^{-2}

Table 4. Evaluation methods of electrical properties of isolated carbon nanotubes and nanocomposites containing CNTs.

Method / Researcher	Experimental	Theoretical				
		Theory	Electrical circuit modeling		modeling	Brownian dynamics simulations (BDS)
			isolated CNT SWCNT	CNT-based composite (Semi empirical)	Probabilistic method	
[10-15, 34]	■					
[8, 15, 21, 34, 44]		■				
[41, 42, 44]			■			
[16-19, 54]				■		
[56, 57]					■	
[58]						■

Electrical conductivity of CNT-based composites

Electrical conductivity of CNT-based composites in both DC and AC are presented in Tables 5 and 6, respectively.

A) Direct current electrical conductivity

The majority of investigations are carried out on DC electrical conductivity.

Mamunya et al. [69] in their recent research achieved the electrical conductivity about 1000 S/m and percolation threshold of about 0.396 wt% for the nanocomposite samples. Also Liao et al. [70] achieved the electrical conductivity about 0.75×10^5S/m in the metallic nanocomposite where vinyl ester resin was used with70 wt% graphite and MWCNTs loadings up to 2 phr. Their results showed that increasing the CNT loading up to 1 phr led to the increase in the electrical conductivity and after that it remained almost constant.

Yan et al. [71] investigated effects of length, diameter, concentration, and interface properties of CNT-based composite using the average field theory. When the aspect ratio (M) was greater than 15, the percolation threshold (fc) of the CNT composite was inversely proportional to the CNT aspect ratio [72], i.e., f_c=0.7/M =0.7d/L, which was found by Monte Carlo simulation [73–74].

Table 5. Electrical conductivityof isolated carbonnanotubes.

Researcher	CNT type	Electrical conductivity (S/m)
Grimes et al. [21]	SWCNTs	3×10^4
Sundaray et al. [63]	MWCNTs	10^4
WU et al. [64]	MWCNTs	2×10^4
Kim et al. [65]	CNT	10^5
Ma et al. [66]	SWCNT	10^4 to 10^8
Kuilla et al. [67]	MWCNT	10^5 to 10^7
Lewandowska et al. [68]	Graphene	7200
	Nano sized steel	1.35×10^6

Researchers achieved the DC electrical conductivity of CNT/PMMA composites about 1000 S/m [79], 3000 S/m [78] and 10000 S/m [14]. In some cases, the electrical conductivity increased 10 orders of magnitude higher than that for pure polymer. The level of electrical conductivity for PMMA polymers is about 10^{-7} S/m. Kim et al. [78] obtained 3×10^3S/m electrical conductivity of composite by adding less than 0.4 MWCNT to PMMA. On the other hand, Skakalova et al. [14] with the higher volume fraction of SWCNT reached to higher electrical conductivity, compared to the work of Kim et al. [78] that used MWCNT in fabrication of nanocomposite. Also Grimes et al. [21] used PMMA with 2×10^{-10}S/m and SWCNT with 3×10^4S/m electrical conductivities and achieved the composite with electrical conductivity of about 0.4 with using in-situ polymerization method, which was comparable with the work of Kim et al. [78,79].

The electrical conductivity of nanocomposite containing the insulated polymers such as PMMA and PS [108] with DC electrical conductivity 10000 S/m showed that the highest value of electrical conductivity of nanocomposites was independent of the conductivity of polymers, but ultimately could not be neglected the effects of conductive polymers such as PANI with 3000 S/m [102] and PPY with 4000 S/m [120] in increasing the total electrical conductivity. In more nanocomposites samples with high electrical conductivity, such as [21] with 0.4 S/m, [100] with 200 S/m, [64] with 398 S/m, [104] with 1600 S/m, [117] with 5100 S/m and [120] with an electrical conductivity about 9100 S/m, in-situ polymerization method

Table 6. DC electrical conductivity of CNT-based composites.

Researcher	Matrix	CNT type	CNT weight fraction (wt%)	Method of Processing	Matrix electrical conductivity (S/m)	Composite electrical conductivity (S/m)	f_c (wt%) t
Liu et al. [8]	PU	SWCNT (modified arcing method)	2	Solution	–	2.2×10^{-2}	~0.2
Saini et al. [9]	PS	PANI-MWCNT (CVD)	10 to 30	In-situ oxidative polymerization route	$\approx 10^{-16}$	5.4×10^{-3} to 3.5	0.5
Martin et al. [10]	Epoxy	MWCNT (CVD) d=50, l=43 ±3	0.01	In-situ polymerization	–	10^{-3}	– 8.6×10^{2}
Sandler et al. [11]	Epoxy	MWCNT (CVD) d=50, l= 17±3	1	In-situ polymerization	$\approx 10^{-9}$	2	2.5×10^{-4} 1.2
Moisala et al. [12]	Epoxy	MWCNT	0.5	Experimental	–	4×10^{-1}	–
Kimet al. [13]	PC	MWCNT	5	Experimental	–	6.4×10^{1}	–
Skakalova et al. [14]	PMMA	SWCNT(HiPCO)	10	Experimental	–	10^{4}	–
Grimes et al. [21]	PEMA	SWCNT arc-discharge	≤23	In-situ polymerization	$\approx 2\times10^{-10}$	≈0.4	≈3
Logakis et al. [34]	PET	MWCNT d= 9.5, l= 1	2.5	In-situ polymerization		3×10^{-1}	6×10^{-2}
Sundaray et al. [63]	PMMA	MWCNT	<2	Electrospinning	10^{-12}	5.3×10^{-2}	$<5\times10^{-2}$ –
Wu et al. [64]	PPY	MWCNT (CVD)	≤3	In-situ chemical oxidative polymerization	1.56×10^{2}	$\approx 3.98\times10^{2}$	–
Benoit et al. [75]	PMMA	SWCNT	≤8	Solution mixing	$\approx 5\times10^{-6}$	$\approx 7\times10^{1}$ (8 wt%)	3.3×10^{-1} 2.1
Stephan et al. [76]	PMMA	MWCNT	≤16	Spin coating	$\approx 5\times10^{-11}$	10^{-3} (16 wt%)	≈0.5 –
Fischer et al. [77]	PMMA	SWCNT(HiPco)	≤7	Coagulation method	$\approx 10^{-9}$	$\approx 1\times10^{-2}$ (7 wt%)	≈1 –
Kim et al. [78]	PMMA	MWCNT(CVD)	≤0.4	Solution mixing	$<10^{-7}$	$\approx 3\times10^{3}$ (0.4 wt%)	3×10^{-3} 2.15
Kim et al. [79]	PMMA	MWCNT (CVD)	≤40	Solution mixing/ casting	10^{-7} (0.001 wt%)	10^{3} (0.3 wt%)	$\approx 3\times10^{-3}$ –
Chauvet et al. [80]	PMMA	SWCNT (arc discharge)	10.4	Solution mixing/ casting	–	$\approx 5\times10^{1}$ (10.4 wt%)	4.29×10^{-1} 2.1
Du et al. [81]	PMMA	Purified SWCNT (HiPco)	≤2	Coagulation method	–	$\approx 5\times10^{-3}$	3.9×10^{-1} 2.3
Pötschke et al. [82]	PC	MWCNT d=10-15, l=1-10	≤5	Melt mixing	$\approx 10^{-14}$	≈1 S/m (5 wt%)	1.44 t = 2.1
Ramasubramaniam et al. [83]	PC	PPE: SWCNT (HiPco)	7	Solution mixing	10^{-13}	4.8×10^{2}	5×10^{-2}-10^{-1}
	PS	SWCNT-functional		Experimental		6.89	4.5×10^{-2}
Pötschke et al. [84]	PC	MWCNT (CVD)	3	Extruded	-	5	1 3.8
Pötschke et al. [85]	PC	MWCNT	≤15	Melt extrusion	$\approx 10^{-13}$	≈10	1–1.5
Pötschke et al. [86]	PC	MWCNT	≤15	Melt mixing	$\approx 2\times10^{-13}$	$\approx 1\times10^{3}$	1–1.5
Pötschke et al. [87]	PC	MWCNT (CVD) d=10-15, l=1-10	15	Experimental		10	1 – 2
Kim et al. [88]	Epoxy	SWCNT	≤0.21	High frequency sonication	–	$\approx 1.25\times10^{-3}$	7.4×10^{-2}

Song et al. [89]	Epoxy	MWCNT(CVD)	≤1.5	Solution mixing d= 20, l= 10–50	≈10^{-7}	≈0.5	$5×10^{-1}$
Barrau et al. [90]	Epoxy	SWCNTs/DWCNTs	≤0.4	Solution mixing	10^{-13}	≈10^{-2} (0.4 wt%)	$8×10^{-2}$ 2.28
Gojny et al. [91]	Epoxy	MWCNT	≤0.5	Calendering process	≈10^{-8}	≈10^{-2} (0.5 wt%)	<10^{-1} –
Thostenson et al. [92]	Epoxy	MWCNT d=15 to 20, l > 10	≤5 wt%	Calendering process	≈10^{-15}	≈5×10 (5 wt%)	<10^{-1} –
Wu et al. [93]	Epoxy	MWCNT(CVD) d=20, l=several microns	23.1	Experimental		0.1 In 1 GHz (AC)	-
Huang et al. [94]	Epoxy	SWCNT (Modified arc-discharge)	15	In-situ polymerization	2.44 × 10^{-11}	$2×10^{1}$	$6.2×10^{-2}$ 2.68
						4	$3.18×10^{-1}$ 2.22
Kovacs et al. [95]	Epoxy	MWCNT (CCVD) d_{in}=4, d_{out}=15 l= 15	1	In-situ polymerization	10^{-9}	$4×10^{-1}$	$1.1×10^{-2}$ 1.7
Yu et al. [96]	Epoxy	SWCNT (Arc), Carbon Solutions Inc.	4	Sonicated, stirred		10	$4×10^{-2}$ 1.7
Liu et al. [97]	Epoxy	SWCNT (Arc)	14	Manually mixed		10^{-2}	$6×10^{-1}$
Li et al. [98]	Epoxy	MWCNT (CVD)	1	Sonicated		$2×10^{-2}$	$2.7×10^{-1}$
Deng et al. [99]	PANI	MWCNTs	≤10	In-situ emulsion polymerization	$2.6×10^{-1}$	6.6	–
Long et al. [100]	PANI	MWCNTs	——	In-situ chemical oxidative polymerization	1.1	≈$1.27×10^{2}$	<24.8
Sharma et al. [101]	PANI	MWCNTs	30	solution casting	–	$2.6×10^{-4}$	–
			50			$1.7×10^{-1}$	
Blanchet et al. [102]	PANI	SWCNT	15	Sonicated		$3×10^{3}$	$3×10^{-1}$ 2.1
Dalmas et al. [103]	SBA	Purified MWCNTs	≤5.4	Suspension mixing	≈10^{-11}	≈20	–
Kymakis et al. [104]	PPY	CNTs	≈50	In-situ polymerization	$3×10^{2}$	≈$1.6×10^{3}$	–
Koerner et al. [105]	PU	MWCNT	10 vol%–0.5	solution casting		10^{2}-10^{3}	$5×10^{-3}$
Gryshchuk et al. [106]	VE	MWCNT (CVD)	2	Sonicated, stirred		$4×10^{-2}$	<$5×10^{-1}$
Battisti et al. [107]	UP	MWCNT	0.3	Experimental	–	$1.3×10^{-1}$	$2.6×10^{-2}$
Grossiord et al. [108]	PS	MWCNT (thermal CVD)	2	Experimental		10^{3}	$1.5×10^{-1}$- $2×10^{-1}$
Poa et al. [109]	PS	MWCNT (Arc)	25	Sonicated, hot pressed		$3×10^{2}$	< 12
Li et al. [110]	PVA	MWNT	60	Experimental		100	5–10
Yoshino et al. [111]	PAT	MWCNT (CVD)	35	Sonicated		$5×10^{1}$	12 2.6
Saeed et al. [112]	PCL	MWCNT (CVD) d=10–20, l=10–50	7	Sonicated, stirred		10	1.5
Mitchell et al. [113]	PCL	SWCNT	3	Sonicated		10^{-3}	0.09 1.5
Mierczynska et al. [114]	PE, UHMW	MWCNT (CVD)	1	Sonicated, dry mixed, hot pressed		$5×10^{1}$	0.045 2.6
Lisunova et al. [115]	PE, UHMW	MWCNT (CVD)	0.7	stirred		10^{-1}	0.14 1.8

Zhao et al. [116]	PVDF	MWCNT (CVD) d= 10–50, l= 4 to 10	2	In-situpolymerization	3×10^{-10}	10	<0.07
				Sonication			
Mclachlan et al. [117]	PI	SWCNT(HiPco) d=0.9–1.2, l=3	-	Shear	6.3×10^{-15}	8.9×10^{3}	5×10^{-4}
				Sonication		3.2×10^{2}	5.06×10^{-4}
				In-situ polymerization		5.1×10^{3}	5.55×10^{-4}
Kilbride et al. [118]	PVA	SWCNT	-	Sonication spin casting	$\approx10^{-10}$	2×10^{-3}	2.9×10^{-4}
Barrau et al. [119]	Epoxy	SWCNT	-	Shear in-situ polymerization	$\approx10^{-14}$	7×10^{-2}	3×10^{-3}
Wu et al. [120]	PPY	MWCNTs	1	In-situ chemical oxidation polymerization		40×10^{2}	
						With coating 0.5 % PSS/ pyrrole monomer 91×10^{2}	
Li et al. [121]	PEDOT: PSS	MWCNT	0	spin coating		2.80	
			0.2			9.16	
Hermant et al. [122]	PEDOT: PSS	SWCNTs (HiPCO)	2.2	In-situ reduction		100	0.32
Gryshchuk et al. [123]	VE	MWCNTs (CVD)	0.5	sonication	10^{-10}	1.94×10^{-4}	----
	VE		1			2.94×10^{-2}	
	VE		2			4.05×10^{-2}	
	VEUH		0.5			1.30×10^{-4}	
	VE/EP		0.5			3.84×10^{-2}	
Wang et al. [125]	Epoxy	SWCNTs	0.5-7	solution casting	----	9×10^{-11}_1.5×10^{-6}	----
Shafi Ullah Khan[126]	Epoxy	MWCNTs	0.05 Random	sonication	----	10^{-7}	----
			0.05 Parrallel to alignment			10^{-5}	
			0.05 Prependicular to alignment			10^{-6}	

has been used for fabrication. As it can be understood from Table 6, the percolation threshold of CNT/epoxy has been reported from 0.0025 wt% to 1 w% based on the CNT type and fabrication process.

The use of CNTs with high aspect ratios have led to a good dispersion of CNT in polymers at low concentration. This subject has been studied by Thostenson et al. [124]. Recent studies show that the electrical properties of CNT-based composites depends strongly on factors such as polymer matrix, method of processing, types of CNT and especially CNT alignment[125,126]. Through aligning CNTs, Khan et al. [126] achieved electrical conductivities from 10^{-7} S/m for composites with random orientation CNTs inside the polymer to 10^{-5} S/m for the CNT/polymer nanocomposites with parallel orientation CNTs aligned into the polymer. Different results on the CNT-based composites originated from different employed materials and measurement techniques are reported.

B) Alternative current electrical conductivity

An overview of experimental studies on AC electrical conductivity of CNT-based composites is presented in Table 7 [10, 34, 55, 65, 117, 127,128].

We investigated the real part of complex electrical conductivity in frequency range of 10^{-2}-10^{6} Hz at room temperature (Table 7). In all nanocomposite samples the phase lag between the measured impedance and AC voltage used at low frequencies was negligible. So, the impedance at 0.01 Hz frequency was equal to the direct current (dc) resistance and the percolation threshold was reported to be about at this frequency.

According to equation 1, the AC electrical conductivity is directly related to the permittivity and frequency, and increases by increasing them [6]. Zhi Hua et al. [127] investigated that by increasing frequency from 0.3 to 18 GHz, both the real and imaginary parts of AC electrical conductivity are increased, but the increase in the electrical conductivity by increased frequency, does not have any practical benefit.

In the research done by Slepyan et al. [129], the properties of CNT-based composites in the terahertz frequency range were studied. They had compared the results obtained from the theoretical study with the experimental observations, and reported a slight difference in a wide range of frequency and temperature.

AC electrical conductivity and complex permittivity can be calculated using equation 12:

$$Z^* = \frac{U^*}{I^*} \tag{12}$$

Permittivity of CNT-based films and composites

CNT films have outstanding electromagnetic properties. For example, well aligned CNT films have an effective and reduced complex permittivity function [130]. Several articles have studied the complex permittivity of different types of carbon nanotubes at low frequencies (upto1GHz). The experimental results on the permittivity of CNT-based composites are shown in Table 8. Wu et al. [93] reported the extreme dependence of the permittivity on the concentration of CNTs in the polymer matrix. In general, the permittivity of homogeneous and isotropic materials is a function of frequency and temperature [131,132]. Complex permittivity of MWCNT composites is extracted as a function of frequency [133].

Watts et al. [134] found that the real part of complex permittivity of defective CNTs in polystyrene films was higher than that of graphite nanotubes at X-band frequency. Grimes et al. [135] fabricated the SWCNTs-based composite with dimensions of about 2×5×0.5 (mm) using the SWCNTs with aspect ratio about 100. It was observed that the dielectric response was very sensitive to the concentration of metallic CNTs and the permittivity of about 100 was achieved. Both theoretical and experimental methods imply that the percolation threshold strongly depends on the aspect ratio and filler particles [136, 137].

Wu et al. [93] studies showed an extremely dependence of real and imaginary parts of relative permittivity on the frequency and concentration of CNTs in the polymer matrix. They prepared samples through addition of MWCNTs between 0.5 to 25.9 volume fraction in an epoxy polymer in frequency range of 10 MHz to 20 GHz, and found that both parts of relative permittivity at megahertz frequency were very high but at gigahertz frequency they showed extremely low values.

The results of experimental studies performed on the permittivity of CNT-based composite are given in Table 8 [7-9,21,55,65,93,94,101,127,133,134,138-146].

Both real and imaginary parts of complex relative permittivity of CNT-based composites are functions of frequency. At low frequencies, the permittivity of CNT-based composites is very high. Grimes et al. [21] with SWCNT/PEMA composites in frequency range between 0.5 to 5.5 GHz with 23% CNT weight fraction reached to the permittivity with real and imaginary parts of between 135 to -27 and 300 to 40, respectively. Also, for MWCNT/PVDF composites having 1% CNT weight fraction in frequency range between 0.1×10^{-6} to 1×10^{-3} Hz , Ghallabi et al. [147] obtained the permittivity with the real part of about 3700 to 6500 at 20°C. For having a nanocomposite with high electrical properties, a low permittivity, especially in its imaginary part, is needed. In most of nanocomposites the imaginary part of permittivity is smaller than its real part [8, 94, 134, 143]. Whereas, according to equation 6, the increase of the loss factor (imaginary part of permittivity ε) of nanocomposites leads to materials with high absorption properties. Nanocomposites with high absorption properties are not suitable for use in electromagnetic waves reflector structures. Although, Huang et al. [94] showed that the imaginary part of permittivity could be higher than its real part for a high content of SWCNT (15 wt%) in epoxy resin in frequency range between 8.2 to 12.4 GHz. Also, they found that tan(δ)=1.42, a more appropriate value compared to that for other samples of nanocomposites.

Table 7. AC electrical conductivity of CNT-based composites.

Researcher	Matrix	CNT type	CNT weight fraction (wt%)	method of Processing	Frequency	Composite complex conductivity (S/m) real	Composite complex conductivity (S/m) imaginary	Year
Martin et al. [10]	Epoxy	MWCNTs (CVD) d=50 nm, l=43±3 um l/d=340	0.01	In-situ polymerization	1 to 10^5 Hz	2.5×10^{-9} to 5×10^{-5} (room temperature)		2004
						3×10^{-4} (80°c)		
						3×10^{-3} (140°c)		
Logakis et al. [34]	PET	MWCNT	0	In-situ polymerization	10^{-1} to 10^6 (Hz)	6×10^{-12} to 8×10^{-13}		2010
			0.5			8×10^{-3} to 1×10^{-2}		
			2.5			6×10^{-1}		
Kim et al. [65]	PDDA	MWCNT	0	---	10^{-3} to 1.8	2×10^{-4} to 3×10^{-1}		2006
			0.5			4×10^{-4} to 3.5×10^{-1}		
			1			9×10^{-4} to 6×10^{-1}		
			2			5×10^{-3} to 8×10^{-1}		
			3			2×10^{-2} to 1		
			4			1×10^{-2} to 0.5		
			5			3×10^{-2} to 1		
			8			2.5 to 10		
Mclachlan et al. [117]	PI	SWCNT (HiPco) d= 0.9–1.2 l=~3	0	In-situ polymerization	10^{-2} to 10^6 Hz	~0.5×10^{-15} to $\times 10^{-7}$		2005
			0.5			~2×10^{-5} to8×10^{-5}		
			1			~2×10^{-4}		
			2			~10^{-3}		
			5			~5×10^{-3}		
ZhiHua et al. [127]	PEMA	SWCNT	4	Theoretically	3×10^{-1} to 18 GHz	1.08×10^{-1} to 5.50	8.1×10^{-2} to 4.11	2008
			8			$<$ 1.25 to 5.25	$<$ 1.25 to 6.6	
			10			$<$ 1.25to 5.90	$<$ 1.25 to 7.2	
			13			$<$ 1.25 to 7.12	$<$ 1.25 to 8.15	
Barrau et al. [128]	Epoxy	MWCNT	2.5	In-situ polymerization	10^{-2} to10^6 Hz	1×10^{-2}		2003
Rafiee et al. [55]	EP/VE	MWCNT (CVD)	0.3	In-situ polymerization	12.4 to 18 GHz	1.99 to 2.2		2014
			0.5			2.27 to 2.7		
			1			2.62 to 3.1		
			1.5			3.65 to 4.7		
			2			4.14 to 5.5		
			2.5			6.2 to 8.6		
			3			8.27 to 11.3		

In the samples having 3% volume fraction of CNTs fabricated by Liu et al. [138] at frequency of 1 GHz, the real and imaginary parts of relative permittivity improved with change in the types of CNTs (single, double and multi-walled) and diameter. For the mixture of silicone and toluene with SWCNTs with diameters between 1 to 2 nm, they reported the values of 16 and 18, respectively, for the imaginary and real parts of permittivity. The imaginary and real parts of permittivity for DWCNTs with diameters between 2 to 4 nm, were 33 and 32 and for MWCNTs with diameters between 8 to 15 nm, were 400 and 360, respectively. According to equation 6, the loss tangents of these samples were found to be 0.571, 1.031 and 1.111, respectively. Also, the dielectric dissipation factor for the sample with combination of the CNTs/epoxy was reported to be 0.44 to 0.45 [144].

The loss tangent for the MWCNTs/PVC nanocomposite having 5% volume fraction of MWCNT at frequency 12.4 GHz was reported to be about 0.071

Table 8.complex relative permittivity of CNT-based composites.

Researcher	Matrix type	CNT type	Max Conductivity (S/m)	CNT weight fraction (wt%)	Method	frequency (GHz)	Complex relative permittivity		Year
							Real (e_r p-p)	Imaginary (e_t p-p)	
Chin et al. [7]	PVA	MWCNTs(^)	-	-	-	0.75–1.5	275 to 195	-	2011
		MWCNTs (Random)	-	-		0.75–1.5	130 to 75	-	
		MWCNTs (çç)	-	-		0.75–1.5	>60	-	
Liu et al. [8]	PU	SWCNT	2.2	0	Solution	8.2-12.4	~2	~0	2007
				5			~7	~2	
				10			~17 to 19	~9 to 11	
				15			~30 to 32	~17 to 22	
				20			32 to 38	~24 to 26	
Saini et al. [9]	PS	PANI coated MWCNT (CVD)	-	10 to 30	In-situ oxidative polymerization route	12.4 to18.0	19 to 44	31 to 87	2011
Grimes et al. [21]	PEMA	SWCNT arc-discharge	-	0	Manually mixed	0.5 to 5.50	~2.5	~2	2007
				4			~9 to 6	~5	
				8			~20 to 10	~14 to 8	
				10 experiment			~25 to 10	~20 to 14	
				10 theory			~23 to 15	~120 to 16	
				13			~63 to 3	~105 to 38	
				15			~80 to -7	~130 to 35	
				18			~115 to -15	~205 to 40	
			~0.4	23 experiment			~135 to -27	~300 to 40	
				23Theory			~100 to -18	~420 to 50	
Kim et al. [65]	PDDA	MWCNT (CVD)	-	0 to 8	Solution	0.001 to 1.8	3 to 440	0.1 to 2×10^4	2006
Wu et al. [93]	Epoxy	MWCNT	-	4.7		3 to 18	5	0.7 to 1.5	2004
				11.4			14 to 20	4 to 7.5	
Huang et al. [94]	Epoxy	SWCNT (modified arc-discharge)	-	0.5	—	8.2 to 12.4 X-band	~6	~1	2007
				1			~7.5	~3	
				3			~17 to 15	~10 to 7	
				5			~28 to 22	~19 to 14	
				10			~40 to 34	~29 to 24	
			20	15			~67 to 42	~75 to 60	
Sharma et al. [101]	PANI	CNTs	2.6×10^{-4}	30	Solution casting	8.0–12.0	14.25 to 11.59	5.7 to 5.79	2009
		CNTs	1.7×10^{-1}	50			39.12 to 33.34	23.47 to 25.34	
		-	-	0			3.87 to 3.25	0.52	
ZhiHua et al. [127]	PEMA	SWCNT	-	4	Theory	0.30 18	6.45 to 5.50	4.87 to 4.11	2008
				8			6.6 to 9	4.15 to 4.85	
				10			7.15 to 10.7	5.9 to 9.1	
				13			8.15 to 13.7	7.2 to 12.30	
Liu et al. [138]	Silicone and Toluene	SWCNTs	-	1	Sonication	0.001 to 1	~6 to 7	~0.2	2010
				2			~9 to 17	~0.8 to 5	
				3			~13 to 28	~1.5 to 16	
				4			~48 to 17	~46 to 2.6	
				5			~24 to 100	~6.5 to 200	

Liu et al. [138]	Silicone and Toluene	DWCNTs	-	1	Sonication	0.001 to 1	~5.4	~0.8	2010
				2			~9 to 14	~0.7 to 2	
				3			~11 to 32	~2 to 33	
				4			~18 to 95	~180 to 4.8	
				5			~20 to 130	~250 to 6	
Liu et al. [138]	Silicone and Toluene	MWCNTs	-	1	Sonication molding	0.001 to 1	~9	~0.2 to 0.3	2010
				1.5			~13 to 19	~1 to 2	
				2			~7 to 40	~2.5 to 30	
				3			~32 to 360	~17 to 400	
				4			~75 to 500	~50 to 280	
Tianjiao et al. [139]	Epoxy	MWCNTs (CVD)	-	0	—	8.2 to 17.8	~3	~0.08 to 0.11	2011
				0.5			~3.5	-	
				1			~4	~0.08 to 0.11	
				2			~5.4 to 7.8	~0.15 to 0.22	
Tianjiao et al. [142]	Epoxy	Cobalt-MWNTs (CVD)	-	0	—	8.2 to 17.8	~2.95 to 3.03	~3.02 to 3.05	2011
				0.5			~3.02 to 3.05	~0.08 to0.11	
				1			~3.05 to 3.13	~3.02 to 3.05	
				2			~3.18 to 3.34	~0.11 to 0.15	
Imai et al. [143]	Cellulose composite papers	MWCNT	0.05	0.5	Suspension mixing	18 to26.5 K-band	-	-	-
			1.5	1			-	-	
			38	2.4			30 to 38	0 to 7	
			150	4.8			38 to 54	68 to 83	
			370	9.1			28 to 112	145 to 193	
			671	16.7			144 to 222	212 to 286	
Watts et al. [134]	PS	MWCNT	-	1:4 ratio films	Polymerization	8 to 12 X- band	8.5 to 9.35	0.05 to 0.18	2003
				1:4			118 to 60	0.36 to 1.1	
				1:6			45 to 17	0.5 to 1.28	
				1:8			27 to 14	0 to 0.3	
Shen et al. [140]	-	MWCNT With Iron (nanogranule)-coated	-	-	Pyrolysis of carbonyl	2	12	2.04	2005
						2 to 18	12 to 4. 7	0.65 to 3.5	
Hou et al. [141]	(PVC)	MWCNTs	-	5:100	-	8.2 to 12.4	~9 to 7	~1.75 to 0.5	2012
				8:100			~10 to 7	~2 to 0	
				10:100			~10 to 13.6	~2.5 to 3.8	
				12:100			~14 to 9	~4.9 to -1.8	
Hou et al. [141]	(PVC)	cobalt:MWCNTs	-	Co:MWCNTs:PVC 0.2:5:100	-	~8.2 to 12.4	~5.9 to 6.9	~2.3 to 3	2012
Hou et al. [141]	(PVC)	La:MWCNTs	-	La:MWCNTs:PVC 0.2:5:100	-	~8.2 to 12.4	~12 to 10.35	~5.25 to 4	2012
Hou et al. [141]	(PVC)	Ni:MWCNTs	-	Ni:MWCNTs: PVC 0.2:5:100	-	~8.2 to 12. 4	~7.3 to 5.5	~3.2 to 2.2	2012
Al Moayed et al. [146]	-	SWCNT	-	-	-	8 to 40 X, Ku, K, Ka	~80 to 20	~200 to 50	2007
Al Moayed et al. [146]	-	MWCNT	-	-	-	8 to 40 X, Ku, K, Ka	~20 to 14	~70 to 15	2007
Kim et al. [139]	Epoxy/ E-glass fibers	CNT (Thermal CVD process)	-	1	Roll milling	8.2 ~ 12.4	6.3	1.2	2010
				2			9 to 9.5	4 to 4.5	
				3			17.1 to 18.9	17.5 to 22	
				4			26.7 to 29.7	40.5 to 50	

Kim et al. [142]	Epoxy/ E-glass fibers	CNT (Thermal CVD process)	-	0.5	Roll milling	8.2 ~ 12.4	7.4 to 7.8	2 to 2.2	2010
				0.75			9 to 9.5	4.1 to 5.2	
				1			13.3 to 15.2	13.7 to 17.4	
				1.5			25.5 to 28	35.2 to 45.2	
Challa et al. [133]	Nylon 6,6 t=2.0 cm w=30 cm	MWCNT	-	1.25	Melt extrusion	8–10	5	1	2008
				2.5			9	2.5	
				5			14 to 15.5	5	
				10			25 to 27	16	
				20			47.5 to 54	58 to 75	
Zhao et al. [144]	Epoxy	MWCNT	-	10	—	8.2 ~ 12.4	13.85 to 14.87	5.85 to 6.47	2008
Han et al. [145]	—	MWCNT (CVD)	-	0	—	1 to 14	4.5 to 5.5	0 to 0.5	2011
				5.2			20 to 48	6 to 24	
				10.4			15 to 85	30 to 162.5	
Ghallabi et al. [147]	PVDF	MWCNT	-	1	Mixing and melting	0.1×10^{-6} to 1×10^{-3}	1800 to 3000 in -50ºC	-	2010
		Barium titanate		20			3700 to 6500 in 20ºC	-	
							4650 to 9900 in 100ºC	-	
							4600 to 10900 in 120ºC	-	
Rafiee et al. [55]	EP/VE	MWCNT (CVD)	–	0.3	In-situ polymerization	12.4 to 18	3.9 to 3.2	2.9 to 2.2	2014
				0.5			4.3 to 3.95	3.3 to 2.7	
				1			6.3 to 5.7	3.8 to 3.1	
				1.5			7.2 to 6.8	5.3 to 4.7	
				2			8.8 to 7.4	6 to 5.5	
				2.5			11.5 to 10.5	9 to 8.6	
				3			14.6 to 13.7	12 to 11.3	

[138], for the SWCNT/epoxy nanocomposite was 0.636 [94], for the SWCNT/PEMAnanocomposite with 4% volume fraction of SWCNT was about 0.833 [62] and for the MWCNT/epoxy/E-glass fibers with 4% volume fraction of MWCNT was found to be 1.683 [139]. Grimes et al. [21] also for the SWCNT/PEMA nanocomposite with 13% volume fraction of reinforcement reported a high loss tangent about of 12.66.

In another research, by incorporation of 3 wt% of multi-walled CNTs into vinyl ester resin the real part and imaginary part of permittivity at 12.4 GHz frequency were obtained 14.6 and 12, respectively [55].

Permeability of CNT-based composites

Experimental observation on the permeability of CNT-based composites is shown in Table (9) [7, 9, 139-141, 144, 145]. Permeability can lead to a decrease in skin depth and reflection losses [9]. Chin et al. [7] obtained the real part of permeability nearly constant and equals 1 in the frequency domain between 0.75 and 1.5 GHz, where CNTs were aligned in the electric field. The permeability of investigated materials increased, respectively, only 0.13 and 0.1 for the vertical and random arrangements of CNTs. The samples with the permeability about 1 are known as materials with non-magnetic properties.

Zhao et al. [144] reported the range of 0.06 to 0.11 for the magnetic dissipation factor ($tg\delta\mu=\mu'\mu''$) at X-band frequency.

According to the results presented in Table (9), the CNT-based composites are materials with low magnetic properties.

CONCLUSION

The influence of some factors, including CNT type (SWCNT, DWCNT and MWCNT), chirality (arm-

Table 9. complex relative permeability of CNT-based composites.

Researcher	Matrix		CNT weight fraction (wt%)	Frequency (GHz)	Complex relative permeability		Year
	Matrix type	CNT type			Real (e_r p-p)	Imaginary (e_t p-p)	
Chin et al. [7]	PVA	MWCNTs (^)	-	0.75–1.5	1	-	2011
	PVA	MWCNTs (Random)			1.1	-	
	PVA	MWCNTs (||)			1.13	-	
Tianjiao et al. [139]	Epoxy	MWCNTs CVD	0	8.2 to 17.8	~3	~0.08 to 0.11	2011
			0.5		~3.5	-	
			1		~4	~0.08 to 0.11	
			2		~5.4 to 7.8	~0.15 to .22	
Tianjiao et al. [139]	Epoxy	Co-MWNTs CVD	0	8.2 to 17.8	~2.95 to 3.03	~3.02 to 3.05	2011
			0.5		~3.02 to 3.05	~0.08 to0.11	
			1		~3.05 to 3.13	~3.02 to 3.05	
			2		~3.18 to 3.34	~0.11 to 0.15	
Shen et al. [140]	-	MWCNT With Iron (nanogranule)-coated	-	2	2.64	1.63	2005
Shen et al. [140]	-	MWCNT With Iron (nanogranule)- coated	-	2 to 18	2.62 to 0.75	1.62 to 0.4	2005
Hou et al. [141]	(PVC)	MWCNTs	5:100	8.2 to 12.4	~1 to 1.2	~0 to 0.2	2012
			8:100		~1.58 to 1.22	~0.05 to 0.33	
			10:100		~1.25 to 1.05	~-0.1 to 0.17	
			12:100		~1.52 to 1.16	~0.15 to 0.96	
Hou et al. [141]	(PVC)	Cobalt:MWCNTs	Co:MWCNTs:PVC 0.2:5:100	~8.2 to 12.4	~1.1 to 1.25	~-0.06 to 0.07	2012
Hou et al. [141]	(PVC)	La:MWCNTs	La:MWCNTs:PVC 0.2:5:100	~8.2 to 12.4	~1.46 to 0.96	~-0.1 to 0.18	2012
Hou et al. [141]	(PVC)	Ni:MWCNTs	Ni:MWCNTs:PVC 0.2:5:100	~8.2 to 12.4	~1.2 to 1.4	~0.05 to 0.16	2012
Saini et al. [9]	Ps	PANI coated MWCNT (CVD)	10 to 30	12.4 to18.0	1.01 to 1.2	0.05 to 0.6	2011
Zhao et al. [144]	Epoxy	MWCNT	10	8.2 ~ 12.4	1.02 to 1.14	0.07 to 0.11	2008
Han et al. [145]	---	MWCNT (CVD)	0	1 to 14	0.9 to 2.5	0.4 to 0.8	2011
			5.2		0.9 to 2.6	0.4 to 1.1	
			10.4		0.5 to 2.5	0.7 to 1.1	

chair, zigzag and chiral), dimension (diameter, length and aspect ratio), structure (metallic or semiconducting), method of CNTs production (CVD, arc-discharge, hipco and etc.), method of processing (solution, melt mixing and in-situ polymerization and etc.), type of polymers (insulating or conductive), volume fraction, CNTs connection in the solution (conductive network), orientation of CNTs in polymer and disentanglement of CNT agglomerates on the electrical and electromagnetic properties of CNT-based composites were discussed. Moreover, in creating the electrical circuits of the CNT-based composites some effective assumptions were considered. With these assumptions, however, researchers proposed equivalent circuits for SWCNTs interconnects, bundle of SWCNTs, DWCNTs and MWCNTs, but they cloud not offer suitable and highly precise electrical models for the CNT nanocomposites.

In contrast to the maturity of conducted simulations on mechanical behavior of CNT-based nanocomposites, a significant lack of simulation activities is identified for the specific aspect of electrical/electromagnetic behavior.

The subjects reviewed in this article indicated that in extracting the electrical properties, most of the researchers used the experimental methods, rather than theoretical, modeling and simulation methods. Consequently, this issue is required to be further addressed in future studies.

In the majority of articles published on CNT-based composites, conductive polymers are less used to fabricate the composites. Although, a higher electrical conductivity was achieved by using insulating polymers instead of conductive polymers, studies on achieving the optimum conditions for constructing conductive CNT nanocomposites with special characteristics are still carrying out.

According to the data extracted from Tables 6-9, the CNT-based composites fabricated by applying the mentioned parameters are good replacements which can be used to make the strong structures with low weight, good conductivity and relative absorption and reflection coefficients. Finally, these materials can be employed as both electromagnetic waves absorbing and reflecting structures.

Besides, it is evident that the influence of functionalization on the electrical/electromagnetic properties of CNT nanocomposites is required to be analyzed more deeply as a challenging issue for future studies.

REFERENCES

1. Iijima S (1991)Helical microtubules of graphitic carbon. Nature 354: 56-58
2. Qing YC, Zhou WC, Luo F, Zhu DM (2010) Electromagnetic and absorbing properties of multi-walled carbon nanotubes/epoxy-silicone coatings. J Inorg Mater 15: 181-185
3. Zhao Y, Yuan L, Duan Y (2010) Study on the electrical behavior of MWCNTs in GF/epoxy composites J Nanosci Nanotechnol 10: 5333-5334
4. Verma P, Saini P, Choudhary V (2015) Designing of carbon nanotube/polymer composites using melt recirculation approach: Effect of aspect ratio on mechanical, electrical and EMI shielding response. J Mater Design 88: 269-277
5. Marconnet AM, Yamamoto N (2011) Nanocomposites with high packing density. J ACS Nano 5: 4818-4825
6. Saini P (2013) Electrical properties and electromagnetic interference shielding response of electrically conducting thermosetting nanocomposites. In: Thermoset nanocomposites. Ed.: Mittal V, Wiley-VCH Verlag GmbH Co. KGaA, Weinheim, Germany, 211-237
7. Chin W, Lu CL, Hsu WK (2011) A radio frequency induced intra-band transition in carbon nanotubes. Carbon 49: 2648-2652
8. Liu Z, Bai G, Huang Y, MaY, Du F, Li F, Guo T, Chen Y (2007) Reflection and absorption contributions to the electromagnetic interference shielding of single-walled carbon nanotube/polyurethane composites. Carbon 45: 821-827
9. Sainia P, Choudhary V, Singhc BP, Mathurc RB, Dhawana SK (2011) Enhanced microwave absorption behavior of polyaniline-CNT/polystyrene blend in 12.4-18.0 GHz range. Synth Met 161: 1522-1526
10. Martin CA, Sandler JKW, Shaffer MSP, Schwarz MK, Bauhofer W, Schulte K, Windle AH (2004) Formation of percolating networks in multi-wall carbon-nanotube-epoxy composites. Compos Sci Technol 64: 2309-2316
11. Sandler JKW, Kirk JE, Kinloch IA, Shaffer MSP, Windle AH (2003) Ultra-low electrical percolation threshold in carbon-nanotube-epoxy composites. Polymer 44: 5893-5899
12. Moisala A, Li Q, Kinloch IA, Windle AH (2006) Thermal and electrical conductivity of single- and multi-walled carbon nanotube-epoxy composites. Compos SciTechnol 66: 1285-1288
13. Kim KH, Jo WH, A strategy for enhancement of mechanical and electrical properties of polycarbonate/multi-walled carbon nanotube composites. Carbon 47: 1126-1134
14. Skakalova V, Dettlaff-Weglikowska U, Roth S (2005) Electrical and mechanical properties of nanocomposites of single wall carbon nanotubes with PMMA. Synth Met 152: 349-352
15. Jun SC, Choi JH (2007) Radio-frequency transmission characteristics of a multi-walled carbon nanotube. Nanotechnology 18: 255701
16. Chen Z, Yu A, Ahmed R, Wang H, Li H, Chen Z (2012) Manganese dioxide nanotube and nitrogen-doped carbon nanotube based composite bifunctional catalyst for rechargeable

zinc-air battery. Electrochim Acta 69: 295-300

17. Qiao Y, Li CMS, Bao J, Bao QL (2007) Carbon nanotube/polyaniline composite as anode material for microbial fuel cells. J Power Sources 170: 79-84
18. Zhang J, Kong LB, Wang B, Luo YC, Kang L (2009) In-situ electrochemical polymerization of multi-walled carbon nanotube/polyaniline composite films for electrochemical supercapacitors. Synth Met159: 260-266
19. Sawatsuk T, Chindaduang A, kung C, Pratontep S, Tumcharern G (2009) Dye-sensitized solar cells based on TiO_2-MWCNTs composite electrodes: Performance improvement and their mechanisms. Diam Relat Mater 18: 524-527
20. Zhao X, Park JY, Huang S, Liu J, McEuen PL (2005) Band Structure, phonon scattering, and the performance limit of single-walled carbon nanotube transistors. Phys Rev Lett 95: 146805
21. Grimes CA, Mungle C, Kouzoudis D, Fang S, Eklund PC (2000) The 500 MHz to 5.50 GHz complex permittivity spectra of single-wall carbon nanotube-loaded polymer composites. Chem Phys Lett 319, 460-464
22. Chung DDL (2001) Electromagnetic interference shielding effectiveness of carbon materials. Carbon 39: 279-285
23. Li N, Huang Y, Du F, He X, Lin X, Gao H, Ma Y, Li F, Chen Y, Eklund P (2006) Electromagnetic interference (EMI) shielding of single-walled carbon nanotube epoxy composites. Nano Lett 6: 1141-1145
24. Park JG, Louis J, Cheng Q, Bao J, Smithyman J, Liang R, Wang B, Zhang C, Brooks J, Kramer L, Fanchasis P, and Dorough D (2009) Electromagnetic interference shielding properties of carbon nanotube buckypaper composites. Nanotechnol 20: 415702-415708
25. Saini P, Choudhary V (2013) Enhanced electromagnetic interference shielding effectiveness of polyaniline functionalized carbon nanotubes filled polystyrene composites. J Nanopart Res 15: 1415
26. Saini P, Choudhary V, Singh BP, Mathur RB, Dhawan SK (2009) Polyaniline-MWCNT nanocomposites for microwave absorption and EMI shielding. Mater Chem Phys 113: 919-926
27. Saini P (2015) Intrinsically conducting polymer-based blends and composites for electromagnetic interference shielding: Theoretical and experimental aspects, in fundamentals of conjugated polymer blends, copolymers and composites: Synthesis, properties and applications, John Wiley & Sons, Inc., Hoboken, NJ, USA
28. Saini P, Arora M (2012) Microwave absorption and EMI shielding behavior of nanocomposites based on intrinsically conducting polymers, graphene and carbon nanotubes. In: New polymers for special applications, Ed. De Souza Gomes A, InTech, Croatia, 71-112
29. Zhao T, Hou C, Zhang H, Zhu R, She S, Wang J, Li T, Liu Z, Wei B (2014) Electromagnetic wave absorbing properties of amorphous carbon nanotubes. Sci Rep 4: 5619
30. Li H, Lu W, Li J, Bai X, Gu C (2005) Multichannel ballistic transport in multiwall carbon nanotubes. Phys Rev Lett 95: 86601
31. Yan Q, Wu J, Zhou G, Duan W, Gu B (2005) Ab initio study of transport properties of multiwalled carbon nanotubes. Phys Rev B 72; 155425
32. Chhowalla M, Teo KBK, Ducati C, Rupesinghe NL, Amaratunga GAJ, Ferrari AC, Roy D, Robertson J, Milne WI (2001) Growth process conditions of vertically aligned carbon nanotubes using plasma enhanced chemical vapor deposition. J Appl Phys 90: 5308-5317
33. McEuen PL, Fuhrer MS, Park HK (2002) Single-walled carbon nanotube electronics. IEEE, doi:1536-125X/02
34. Logakis E, Pissis P, Pospiech D, Korwitz A, KrauseB, Reuter U, Potschke P (2010) Low electrical percolation threshold in poly(ethylene terephthalate)/multi-walled carbon nanotube nanocomposites. Eur Polym J 46: 928-936
35. Dosoudil R, Ušák E, Olah V (2010) Automated measurement of complex permeability and permittivity at high frequencies. J Electer Eng 61: 111-114
36. Verma P, Saini P, Malik RS, Choudhary V (2015) Excellent electromagnetic interference shielding and mechanical properties of high loading carbon

nanotubes/polymer composites designed using melt recirculation equipped twin-screw extruder. Carbon 89: 308-317

37. Saini P, Choudhary V, Vijayan N, Kotnala RK (2012) Improved electromagnetic interference shielding response of poly(aniline)-coated fabrics containing dielectric and magnetic nanoparticles. J Phys Chem C 116: 13403-13412
38. Ku H (2003)Curing vinyl ester particle-reinforced composites using microwaves. J Compos Mater, doi: 10.1177/0021998303036266
39. Eda G, Chhowalla M (2009) Graphene-based composite thin films for electronics. Nano Lett 9: 814-818
40. Liu YJ, Chen XL (2003) Evaluations of the effective material properties of carbon nanotube-based composites using a nanoscale representative volume element. Mech Mater 35: 69-81
41. Burke PJ (2003) An RF circuit model for carbon nanotubes. IEEE Trans, doi:10.1109/TNANO.2003.808503
42. Burke PJ (2002) Lüttinger liquid theory as a model of the gigahertz electrical properties of carbon nanotubes. IEEE Trans, doi:10.1109/TNANO.2002.806823
43. Naeemi A, Meindl JD (2006) Compact physical models for multiwall carbon-nanotube interconnects. IEEE Electron Devic L, doi:10.1109/LED.2006.873765
44. Naeemi A, Meindl JD (2007) Design and performance modeling for single-walled carbon nanotubes as local, semiglobal, and global interconnects in gigascale integrated systems. IEEE T Electron Dev, doi:10.1109/TED.2006.887210
45. Nieuwoudt, A, Massoud Y (2006) Evaluating the impact of resistance in carbon nanotube bundles for VLSI interconnect using diameter-dependent modeling techniques. IEEE T Electron Dev, doi:10.1109/TED.2006.882035
46. Massoud Y, Nieuwoudt A (2006) Accurate resistance modeling for carbon nanotube bundles in VLSI interconnect. IEEE Conf Nanotechnology, doi:10.1109/NANO.2006.247631
47. Pu SN, Yin WY, Mao JF, Liu QH (2009) Crosstalk prediction of single- and double-walled carbon-nanotube (SWCNT/DWCNT) bundle Interconnects. IEEE T Electron Dev 56: 560-568
48. de Pablo PJ, Graugnard E, Walsh B, Andres RP, Datta S, Reifenberger R (1999) A simple, reliable technique for making electrical contact to multiwalled carbon nanotubes. Appl Phys Lett 74: 323-325
49. Wei BQ, Vajtai R, Ajayan PM (2001) Reliability and current carrying capacity of carbon nanotubes. Appl Phys Lett 79: 1172-1174
50. Sato S, Nihei M, Mimura A, Kawabata A, Kondo D, Shioya H, Iwai T, Mishima M, Ohfuti M, Awano Y (2006) Novel approach to fabricating carbon nanotube via interconnects using size-controlled catalyst nanoparticles. Interconnect Technol Conf, doi:10.1109/IITC.2006.1648696
51. Bockrath M, Cobden DH, McEuen PL, Chopra NG, Zettl A, Thess A, Smalley RE (1997) Single-electron transport in ropes of carbon nanotubes. Science 275: 1922-1925
52. Naeemi A, Meindl JD (2008) Performance modeling for single- and multiwall carbon nanotubes as signal and power interconnects in gigascale systems. IEEE T Electron Dev 55: 2574-2582
53. Hosseini A, Shabro V (2010) Thermally-aware modeling and performance evaluation for single-walled carbon nanotube-based interconnects for future high performance integrated circuits. Microelectron Eng 87: 1955-1962
54. Chang J, Liang G, Gu A, Cai S, Yuan L (2012) The production of carbon nanotube/epoxy composites with a very high dielectric constant and low dielectric loss by microwave curing. Carbon 50: 689-698
55. Rafiee R, Sabour MH, Nikfarjam A, Taheri M (2014) The influence of CNT contents on the electrical and electromagnetic properties of CNT/vinylester, J Electron Mater 43: 3477-3485
56. Li C, Thostenson ET, Chou TW (2008) Effect of nanotube waviness on the electrical conductivity of carbon nanotube-based composites. Compos Sci Technol 68: 1445-1452
57. Yi YB Berhan L (2004) Statistical geometry of

random fibrous networks, revisited: Waviness, dimensionality, and percolation. J Appl Phys 96: 1318-1327
58. Mendes MJ, Schmidt HK, Pasquali M (2008) Brownian dynamics simulations of single-wall carbon nanotube separation by type using dielectrophoresis. J Phys Chem B 112: 7467-7477
59. Tans SJ, Verschueren ARM, Dekker C (1998) Room-temperature transistor based on a single carbon nanotube. Nature 393: 49-52
60. Prabhakar RB (2007) Electrical properties and applications of carbon nanotube structures. J Nanosci Nanotechnol 7: 1-29
61. Wei BQ, Vajtai R, Ajayan PM (2001) Reliability and current carrying capacity of carbon nanotubes. Appl Phys Lett 79: 1172-1174
62. Solymar L, Walsh D (2004) Electrical properties of materials. Oxford University Press
63. Sundaray B, Subramanian V, Natarajan TS, Krishnamurthy K (2006) Electrical conductivity of a single electrospun fiber of poly (methyl methacrylate) and multiwalled carbon nanotube nanocomposites. Appl Phys Lett 88: 143114
64. Wu TM, Lin SH (2006) Characterization and electrical properties of polypyrrole/multiwalled carbon nanotube composites synthesized by In situ chemical oxidative polymerization. J Polym Sci Pol Phys 44: 1413-1418
65. Kim YJ, Shin TS, Choi HD, Kwon JH, Chung YC, Yoon HG (2005) Electrical conductivity of chemically modified multiwalled carbon nanotube/epoxy composites. Carbon 43: 23-30
66. Ma PC, Siddiqui NA, Marom G, Kim JK (2010) Dispersion and functionalization of carbon nanotubes for polymer-based nanocomposites: A review. Compos Part A 41: 1345-1367
67. Kuilla, T, Bhadra S, Yao D, Kim NH, Bose S, Lee JH (2010) Recent advances in graphene based polymer composites. Prog Polym Sci 35: 1350-1375
68. Lewandowska M, Krawczynıska AT, Kulczyk M, Kurzydłowski KJ (2009) Structure and properties of nano-sized Eurofer 97 steel obtained by hydrostatic extrusion. J Nucl Mater 386-8: 499-502
69. Mamunya Y, Boudenne A, Lebovka N, Ibos L, Candau Y, Lisunova M (2008) Electrical and thermophysical behaviour of PVC-MWCNT nanocomposites. Compos Sci Technol 68: 1981-1988
70. Liao SH, Hung CH, Ma CCM, Yen CY, Lin YF, Weng CC (2008) Preparation and properties of carbon nanotube-reinforced vinyl ester/ nanocomposite bipolar plates for polymer electrolyte membrane fuel cells. J Power Sources 176: 175-182
71. Yan KY, Xue QZ, Zheng QB, Hao LZ (2007) The interface effect of the effective electrical conductivity of carbon nanotube composites. Nanotechnology 18: 255705
72. Balberg I, Binenbaum N, Wagner N (1984) Percolation thresholds in the three-dimentinal sticks system. Phys Rev Lett 52: 1465-1468
73. Lagarkov AN, Sarychev AK (1996) Electromagnetic properties of composites containing elongated conducting inclusions. Phys Rev B 53: 6318-6336
74. Celzard A, McRae E, Deleuze C, Dufort M, Furdin G, Mareche JF (1996) Critical concentration in percolating systems containing a high-aspect-ratio filler. Phys Rev B 53: 6209-6214
75. Benoit JM, Corraze B, Lefrant S, Blau WJ, Bernier P, Chauvet O (2001)Transport properties of PMMA-carbon nanotubes composites. Synth Met 121: 1215-1216
76. Stephan C, Nguyen TP, Lahr B, Blau W, Lefrant S, Chauvet O (2002) Raman spectroscopy and conductivity measurements on polymer-multiwalled carbon nanotubes composites. J Mater Res 17: 396-400
77. Du F, Fischer JE, Winey KI (2003) Coagulation method for preparing single-walled carbon nanotube/poly(methyl methacrylate) composites and their modulus, electrical conductivity, and thermal stability. J Polym Sci Pol Phys 41: 3333-3338
78. Kim HM, Kim K, Lee SJ, Joo J, Yoon HS, Cho SJ, Lyu SC, Lee CJ (2004) Charge transport properties of composites of multiwalled carbon nanotube with metal catalyst and polymer: Application to electromagnetic interference

shielding. Curr Appl Phys 4: 577-580
79. Kim HM, Kim K, Lee CY, Joo J, Cho SJ, Yoon HS, Pejakovic DA, Yoo JW, Epstein AJ (2004) Electrical conductivity and electromagnetic interference shielding of multiwalled carbon nanotube composites containing Fe catalyst. Appl Phys Lett 84: 589-591
80. Chauvet O, Benoit JM, Corraze B (2004) Electrical, magneto-transport and localization of charge carriers in nanocomposites based on carbon nanotubes. Carbon 42: 949-952
81. Du F, Scogna RC, Zhou W, Brand S, Fischer JE, Winey KI (2004) Nanotube networks in polymer nanocomposites: Rheology and electrical conductivity. Macromolecules 37: 9048-9055
82. Pötschke P, Dudkin SM, Alig I (2003) Dielectric spectroscopy on melt processed polycarbonate-multiwalled carbon nanotube composites. Polymer 44: 5023-5030
83. Ramasubramaniam R, Chen J, Liu H (2003) Homogeneous carbon nanotube/polymer composites for electrical applications. Appl Phys Lett 83: 2928-2930
84. Pötschke P, Abdel-Goad M, AligI, Dudkin S, Lellinger D (2004) Rheological and dielectrical characterization of melt mixed polycarbonate-multiwalled carbon nanotube composites. Polymer 45: 8863-8870
85. Pötschke P, Bhattacharyya AR, Janke A, Goering H (2003) Melt mixing of polycarbonate/multi-wall carbon nanotube composites. Compos Interf 10: 389-404
86. Potschke P, Bhattacharyya AR, Janke A (2004) Carbon nanotube-filled polycarbonate composites produced by melt mixing and their use in blends with polyethylene. Carbon 42: 965-969
87. Pötschke P, Fornes TD, Paul DR (2002) Rheological behavior of multiwalled carbon nanotube/polycarbonate composites. Polymer 43: 3247-3255
88. Kim BK, Lee J, Yu I (2003) Electrical properties of single-wall carbon nanotube and epoxy composites. J Appl Phys 94: 6724-6728
89. Song YS, Youn JR (2005) Influence of dispersion states of carbon nanotubes on physical properties of epoxy nanocomposites. Carbon 43: 1378-1385
90. Barrau, S, Demont P, Maraval C, Bernes A, Lacabanne C (2005) Glass transition temperature depression at the percolation threshold in carbon nanotube-epoxy resin and polypyrrole-epoxy resin composites. Macromol Rapid Commun 26: 390-394
91. Gojny FH, Wichmann MHG, Fiedler B, Kinloch IA, Bauhofer W, Windle AH, SchulteK (2006) Evaluation and identification of electrical and thermal conduction mechanisms in carbon nanotube/epoxy composites. Polymer 47: 2036-2045
92. Thostenson ET, Chou TW (2006) Processing-structure-multi-functional property relationship in carbon nanotube/epoxy composites. Carbon 44: 3022-3029
93. Wu J, Kong L (2004) High microwave permittivity of multiwalled carbon nanotube composites. Appl Phys Lett 84: 4956-4958
94. Huang Y, Li N, Ma Y, Du F, Li F, He X, Lin X, Gao H, Chen Y (2007) The influence of single-walled carbon nanotube structure on the electromagnetic interference shielding efficiency of its epoxy composites. Carbon 45: 1614-1621
95. Kovacs JZ, Velagala BS, Schulte K, Bauhofer W (2007) Two percolation thresholds in carbon nanotube epoxy composites. Compos Sci Technol 67: 922-928
96. Yu A, Itkis ME, Bekyarova E, Haddon RC (2006) Effect of single-walled carbon nanotube purity on the thermal conductivity of carbon nanotube-based composites. Appl Phys Lett 89: 133102
97. Liu L, Matitsine S, Gan YB, Chen LF, Kong LB, Rozanov KN (2007) Frequency dependence of effective permittivity of carbon nanotube composites. J Appl Phys 101: 94106
98. Li J, Ma PC, Chow WS, To CK, Tang BZ, Kim JK (2007) Correlations between percolation threshold, dispersion state, and aspect ratio of carbon nanotubes. Adv Funct Mater 17: 3207-3215
99. Deng J, Ding X, Zhang W, Peng Y, Wang J, Long X, Li P, Chan ASC (2002) Carbon nanotube-polyaniline hybrid materials. Eur Polym J 38:

2497-2501
100. Long Y, Chen Z, Zhang X, Zhang J, Liu Z (2004) Synthesis and electrical properties of carbon nanotube polyaniline composites. Appl Phys Lett 85: 1796-1798
101. Sharma BK, Khare N, Sharma R, Dhawan SK, Vankar VD, Gupta HC (2009) Dielectric behavior of polyaniline-CNTs composite in microwave region. Compos Sci Technol 69: 1932-1935
102. Blanchet GB, Fincher CR, Gao F (2003) Polyaniline nanotube composites: A high-resolution printable conductor. Appl Phys Lett 82: 1290-1292
103. Dalmas F, Chazeau L, Gauthier C, Masenelli-Varlot K, Dendievel R, Cavaille JY, Forro L (2005) Multiwalled carbon nanotube/polymer nanocomposites: Processing and properties. J Polym Sci Part Pol Phys 43: 1186-1197
104. Kymakis E, Amaratunga G (2006) Electrical properties of single-wall carbon nanotube-polymer composite films. J Appl Phys 99: 084302-7
105. Koerner H, Liu W, Alexander M, Mirau P, Dowty H, Vaia RH (2005) Deformation-morphology correlations in electrically conductive carbon Nanotube-thermoplastic polyurethane nanocomposites. Polymer 46: 4405-4420
106. Gryshchuk O, Karger-Kocsis J, Thomann R, Konya Z, Kiricsi I (2006) Multiwall carbon nanotube modified vinylester and vinylester-based hybrid resins. Compos A 37: 1252-1259
107. Battisti A, Skordos AA, Partridge IK (2010) Percolation threshold of carbon nanotubes filled unsaturated polyesters. Compos Sci Technol 70: 633-637
108. Grossiord N, Loos J, Laake LV, Maugey M, Zakri C, Koning CE, Hart AJ (2008) High-conductivity polymer nanocomposites obtained by tailoring the characteristics of carbon nanotube fillers. Adv Funct Mater 18: 3226-3234
109. Poa CH, Silva SRP, Watts PCP, Hsu WK, Kroto HW, Walton DRM (2002) Field emission from nonaligned carbon nanotubes embedded in a polystyrene matrix. Appl Phys Lett 80: 3189-3191
110. Li HC, Lu SY, Syue SH, Hsu WK, Chang SC (2008) Conductivity enhancement of carbon nanotube composites by electrolyte addition. Appl Phys Lett 93: 033104
111. Yoshino K, Kajii H, Araki H, Sonoda T, Take H, Lee S (1999) Electrical and optical properties of conducting polymer-fullerene and conducting polymer-carbon nanotube composites. Full Sci Technol 7: 695-711
112. Saeed K, Park SY (2007) Preparation and properties of multiwalled carbon nanotube/polycaprolactone nanocomposites. J Appl Polym Sci 104: 1957-1963
113. Mitchell CA, Krishnamoorti R (2007) Dispersion of single-walled carbon nanotubes in poly(ε-caprolactone). Macromolecules 40: 1538-1545
114. Mierczynska A, Mayne-L'Hermite M, Boiteux G (2007) Electrical and mechanical properties of carbon nanotube/ultrahigh-molecular-weight polyethylene composites prepared by a filler prelocalization method. J Appl Polym Sci 105: 158-168
115. Lisunova MO, Mamunya YP, Lebovka NI, Melezhyk AV (2007) Percolation behaviour of ultrahigh molecular weight polyethylene/multi-walled carbon nanotubes composites. Europ Polym J 43: 949-958
116. Zhao Z, Zheng W, Yu W, Long B (2009) Electrical conductivity of poly(vinylidene fluoride)/carbon nanotube composites with a spherical substructure. Carbon 47: 2112-2142
117. Mclachlan DS, Chiteme C, Park C, Wish KE, Lowther SE, Lillehei PT, Siochi EJ, Harrison JS (2005) AC and DC percolative conductivity of single wall carbon nanotube polymer composites. J Polym Sci Pol Phys 43: 3273-3287
118. Kilbride BE, Coleman JN, Fraysse J, Fournet P, Cadek M, Drury A, Huntzler S, Roth S, Blau WJ (2002) Experimental observation of scaling laws for alternating current and direct current conductivity in polymer-carbon nanotube composite thin films. J Appl Phys 92: 4024-4030
119. Barrau S, Demont P, Peigney A, Laurent C, Lacabanne, C (2003) DC and AC conductivity of carbon nanotubes–polyepoxy composites. Macromolecules 36: 5187-5194
120. Wu TM, Chang HL, Lin YW (2009) Synthesis

and characterization of conductive polypyrrole/ multi-walled carbon nanotubes composites with improved solubility and conductivity. Compos Sci Technol 69: 639-644

121. Li J, Liu J, Gao C, Zhang J, Sun H (2009) Influence of MWCNTs doping on the structure and properties of PEDOT:PSS films. Int J Photoenergy, doi:10.1155/2009/650509
122. Hermant MC, van der Schoot P, Klumperman B, Koning CE (2010) Probing the cooperative nature of the conductive components in polystyrene/ poly(3,4-ethylenedioxythiophene): Poly(styrene sulfonate) single-walled carbon nanotube composites. ACS Nano 4: 2242-2248
123. Gryshchuk O, Karger-Kocsis J, Thomann R, Konya Z, Kiricsi I (2006) Multiwall carbon nanotube modified vinylester and vinylester-based hybrid resins. Compos A-Appl S 37: 1252-1259
124. Thostenson ET, Ren Z, Chou TW (2001) Advances in the science and technology of carbon nanotubes and their composites: A review. Compos Sci Technol 61: 1899-1912
125. Wang Q, Dai J, Li W, Wei Z, Jiang J (2008) The effects of CNT alignment on electrical conductivity and mechanical properties of SWNT/epoxy nanocomposites. Compos Sci Technol 68: 1644-1648
126. Khan SU, Pothnis JR, Kim JK (2013) Effects of carbon nanotube alignment on electrical and mechanical properties of epoxy nanocomposites. Compos A 49: 26-34
127. Zhi Hua P, Jing Cui P, Yan Feng P, Jie Yang W (2008) Complex conductivity and permittivity of single wall carbon nanotubes/polymer composite at microwave frequencies: A theoretical estimation. Chinese Sci Bull 53: 3497-3504
128. Barrau S, Demont P, Peigney A, Laurent C, Lacabanne C (2003) DC and AC conductivity of carbon nanotubes−polyepoxy composites. Macromolecules 36: 5187-5194
129. Slepyan GY, Shuba MV, Maksimenko SA, Thomsen C, Lakhtakia A (2010) Electromagnetic properties of composite materials containing carbon nanotubes. URSI International Symposium on Electromagnetic Theory, doi:10.1109/URSI-EMTS.2010.5637292
130. Kozlowski G, Kleismit R, Boeckl J, Campbell A, Munbodh K, Hopkins S, Koziol K, Peterson T (2009) Electromagnetic characterization of carbon nanotube films by a two-point evanescent microwave method. Physica E 41: 1539-1544
131. Brown WF (1956) Dielectrics, Springer, Berlin, Heidelberg
132. Mangalaraj D, Radhakrishnan M, Balasubramanian C (1982) Dielectric and AC conduction properties of ion plated aluminum nitride thin films. J Phys D Appl Phys, doi:10.1088/0022-3727/15/3/012
133. Challa RK, Kajfez D, Demir V, Gladden JR, Elsherbeni A (2008) Characterization of multiwalled carbon nanotube (MWCNT) composites in a waveguide of square cross section. IEEE. Microwave wireless comp lett 18: 161-163
134. Watts PCP, Ponnampalam DR, Hsu WK, Barnes A, Chambers B (2003) The complex permittivity of multi-walled carbon nanotube-polystyrene composite films in X-band. Chem Phys Lett 378: 609-614
135. Grimes CA, Mungle C, Kouzoudis D, Fang S, Eklund PC (2000) The 500 MHz to 5.50 GHz complex permittivity spectra of single-wall carbon nanotube-loaded polymer composites. Chem Phys Lett 319: 460-464
136. Celzard A, McRae E, Deleuze C (1996) Critical concentration in percolating systems containing a high-aspect-ratio filler. Phys Rev B 53: 6209-6214
137. Munson-McGee SH (1991) Estimation of the critical concentration in an anisotropic percolation network. Phys Rev B 43: 3331-3336
138. Liu L, Kong LB, Yin WY, Chen Y, Matitsine S (2010) Microwave dielectric properties of carbon nanotube composites. Carbon Nanotubes, doi: 10.5772/39420
139. Tianjiao B, Yan Z, Xiaofeng S, Yuexin D (2011) A study of the electromagnetic properties of cobalt-multiwalled carbon nanotubes (Co-MWCNTs) composites. Mater Sci Eng B 176: 906-912
140. Shen X, Gong RZ, Nie Y, Nie JH (2005) Preparation and electromagnetic performance of

coating of multiwall carbon nanotubes with iron nanogranule. J Magn Mater 288: 397-402
141. Hou C, Li T, Zhao T, Zhang W, Cheng Y (2012) Electromagnetic wave absorbing properties of carbon nanotubes doped rare metal/pure carbon nanotubes double-layer polymer composites. Mater Design 33: 413-418
142. Kim JB, Byun JH (2010) Influence of the CNT length on complex permittivity of composite laminates and on radar absorber design in X-band. Nanotechnology, doi: 10.1109/NANO.2010.5697804
143. Imai M, Akiyama K, Tanaka T, Sano E (2010) Highly strong and conductive carbon nanotube/cellulose composite paper. Compos Sci Techno l70: 1564-1570
144. Zhao DL, Li X, Shen ZM (2008) Microwave absorbing property and complex permittivity and permeability of epoxy composites containing Ni-coated and Ag filled carbon nanotubes. Compos Sci Technol 68: 2902-2908
145. Han M, Deng L (2011) High frequency properties of carbon nanotubes and their electromagnetic wave absorption properties. In: Carbon nanotubes applications on electron devices, In Tech.